Supplementary Information for the Effect of land use changes on air quality: Impacts of urbanization, urban vegetation, and agriculture.

Alba Badia[a,b], Ricard Segura-Barrero[a], Sergi Ventura[a], Marc Guevara[b], Josep Peñuelas[c,d], Gara Villaba[a,e]

[a]*Sostenipra Research Group Institute of Environmental Sciences and Technology Universitat Autnoma de Barcelona 08193 Bellaterra Barcelona Spain.*
[b]*Barcelona Supercomputing Center Barcelona 08034 Spain*
[c]*CSIC Global Ecology Unit CREAF-CSIC-UAB 08193 Bellaterra Barcelona Spain.*
[d]*CREAF Universitat Autnoma de Barcelona 08193 Bellaterra Barcelona Spain.*
[e]*Department of Chemical Biological and Environmental Engineering Universitat Autnoma de Barcelona 08193 Bellaterra Barcelona Spain*

Contents of this file:

*Corresponding author: alba.badia@bsc.es

Supplementary Text

S1. Land-use maps

In the REF scenario, the land-use map was derived by combining the Corine Land Cover 2018 map for rural areas[1] and the LCZ map of the AMB [2] for urban areas. This combined map was reclassified to the United States Geological Survey (USGS) land classification following the rules of Pineda et al., (2004)[3]. For the remaining scenarios, we applied a masking technique to the reference map, isolating areas where land-use changes occurred and assigning them the new land-use class. In the case of urban fraction, a reference map was generated utilizing the annually maximum NDVI at a 30 m resolution, to differentiate the areas with vegetation from urbanization, as it is described in Segura et al., 2021[4]. In subsequent scenarios, adjustments were made to the REF urban fraction map, specifically in regions where land-use changes deviated from the REF scenario. If the new land-use pertained to rural or urban park class, it was masked as 0. Conversely, if the new land-use was urban, the urban fraction was calculated based on the mean for the corresponding LCZ and applied to the urban fraction mask.

S2. Agriculture and urban parks irrigation water use estimation

Monthly irrigation water use estimates for 2015 considered in this study, are calculated which different methodologies for agriculture and urban parks.

In agriculture, a water metabolism approach is used to determine monthly water requirements at the parcel level. Every crop is given a monthly coefficient using the land-use map, which is determined by the local farmer's calendar and literature. An adaption of the FAO approach is used to obtains the crop water requirement in mm per month[5]. The crop's coefficients, observed evapotranspiration and precipitation interpolated maps, and irrigation efficiencies provided in Agència Catalana de l'aigua (2010)[6] are used to create monthly raster maps of irrigation water use. For urban parks and gardens, the AMB reports that the maximum application rate to irrigated areas in summer is 2.5 l $m^{-2}day^{-1}$, equivalent to 13% of park expansion[7]. In other months, irrigation is reduced according to a schedule reported by the Ajuntament de Barcelona (2013)[8]. Vegetation areas in built-up areas and urban park areas define irrigation areas. The two irrigation data sets were merged and resampled at a resolution of 100 m.

S3. Model validation

The simulation of the reference scenario was evaluated with observational data from the Catalan Meteorological Service (SMC) and the Spanish Meteorological Agency (AEMET) of the AMB (see Supplementary Table S2). The variables assessed included temperature, relative humidity, wind speed, and wind direction. The details of the 19 meteorological stations used here are provided in Segura et al., (2021)[4]. The model's hourly data was compared with the corresponding observational hourly data, and the average value for each statistic was computed for each station. Overall, the model shows strong agreement with the observed temperatures and relative humidities, with correlation coefficients ranging from 0.85 to 0.98 for temperature and 0.51 to 0.91 for relative humidity. The root-mean-square errors (RMSE) for temperature are 1.4 ^{o}C for urban and rural stations, both of which are lower than those reported in previous studies for the AMB during the same period (RMSE = 1.6 ^{o}C in Segura et al., (2021)[4]), indicating a good model performance. For wind speed, the model also demonstrates a strong correlation with observations, with coefficients between 0.65 and 0.91. However, a specific bias was observed in urban areas (NMB = -0.34). This bias may stem from the challenges of comparing local wind conditions, which are influenced by complex urban topography—such as meteorological stations located on building rooftops—with a mesoscale model that has a relatively coarse resolution of 1 km. In terms of wind direction, the WRF-Chem model shows the lowest correlations with observations among the four variables examined, with correlation coefficients ranging from 0.16 to 0.88. Additionally, the root-mean-square errors are high (RMSE = 55.3^{o} for urban stations and 43.0^{o} for rural stations), highlighting the limitations of the mesoscale model in accurately capturing local-scale wind directions. Even though, there is no specific bias in the wind direction.

In addition, the reference scenario was evaluated with air quality observation data publicly available from the Xarxa de Vigilància i Previsió de la Contaminació Atmosfèrica (XVPCA) of the AMB for NO_2, O_3 and PM10 (see Figure 1 in the main text and Supplementary Table S3). The modelled concentrations were converted to units of µg m^{-3} using the temperatures and pressures from the model output. Overall, the model shows good agreement with the observations during the period of July 2015 (correlations between 0.1-0.68, 0.54-0.77 and 0.1-0.3, for NO_2, O_3 and PM10, respectively), although there are specific biases (NMB=0.14, 0.13 and 0.6, for NO_2, O_3 and, PM10 respectively) over the urban stations representing high traffic (urban

traffic). However, the model exhibits low biases (NMB=0.001 and 0.06, for NO_2 and O_3, respectively) at stations located in low traffic areas (urban background stations). The surface NO_2, O_3 and PM10 concentrations in high traffic areas are very sensitive to traffic emissions. Therefore, these model biases are mostly due to limitations in the emission inventory, including the nonconsideration of congestion effects, as shown by Rodríguez-Rey et al. (2021)[9] and the resolution of our model (1km), which is not able to capture traffic hotspots. Furthermore, the PM10 underestimation could also be attributed to dust episodes occurred in July 2015 that the model is not able to capture[10].

Validating the model for NH_3 concentration is essential when assessing the impact of agriculture on air quality. Unfortunately, NH_3 observational data are not available for our domain and the period of analysis. However, NH_3 concentrations in our model, ranging from 1 to 11 µg m^{-3}, are in agreement with other studies, such as Reche et al. (2022)[11], which measure the 2011–2020 trends of urban and regional ammonia in and around Barcelona.

Supplementary Figures

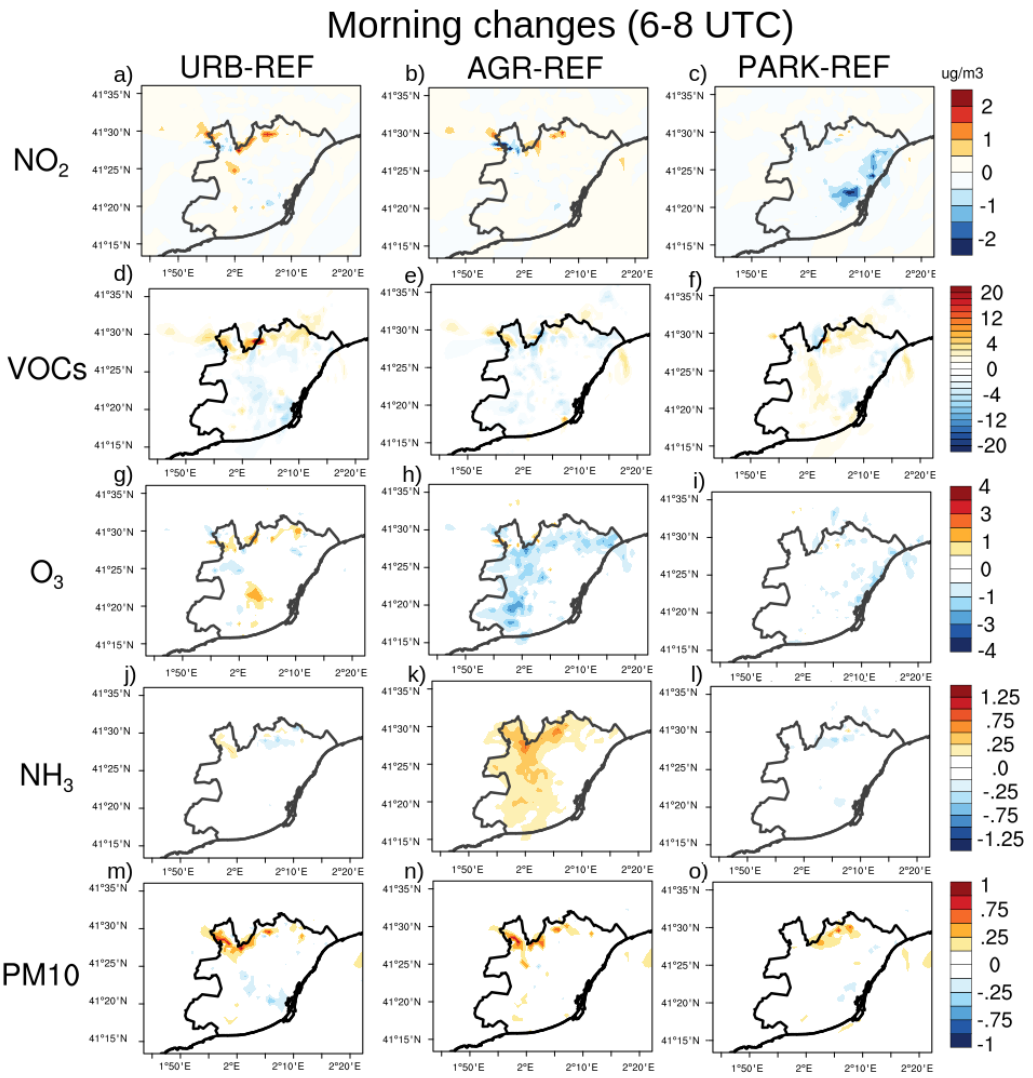

Figure S1: Morning (6-8 UTC) air quality average changes (in µg m^{-3}) due to the increase of urbanization (URB-REF), agriculture (AGR-REF) and urban parks (PARK-REF) for a period before the heatwave.

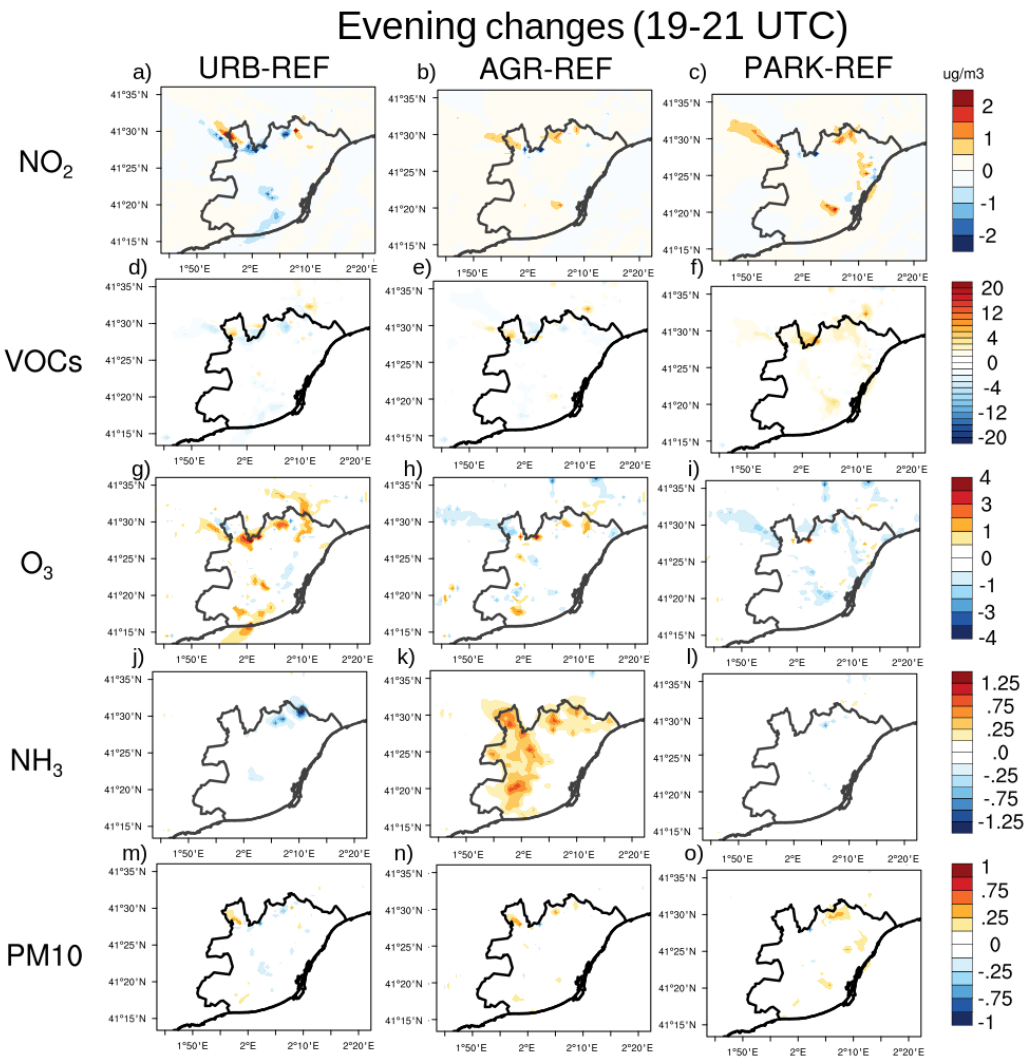

Figure S2: Evening (19-21 UTC) air quality average changes (in µg m^{-3}) due to the increase of urbanization (URB-REF), agriculture (AGR-REF) and urban parks (PARK-REF) for a period before the heatwave.

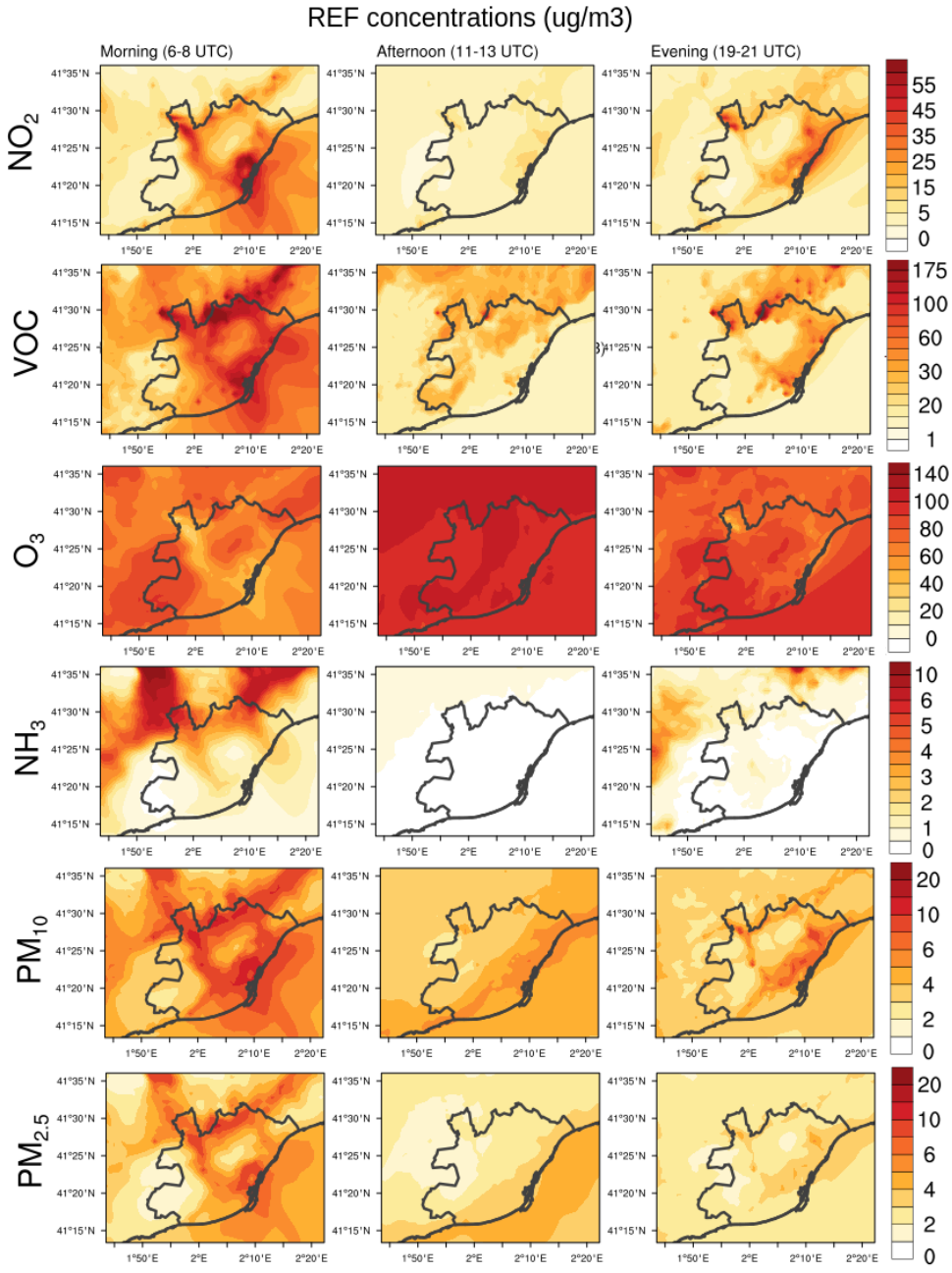

Figure S3: Air quality in the reference scenario (REF).

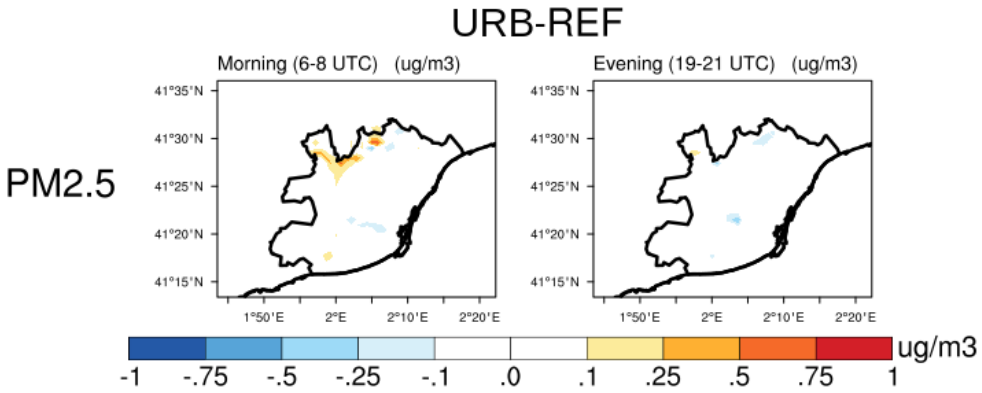

Figure S4: PM2.5 changes due to the increase on urbanization (URB-REF).

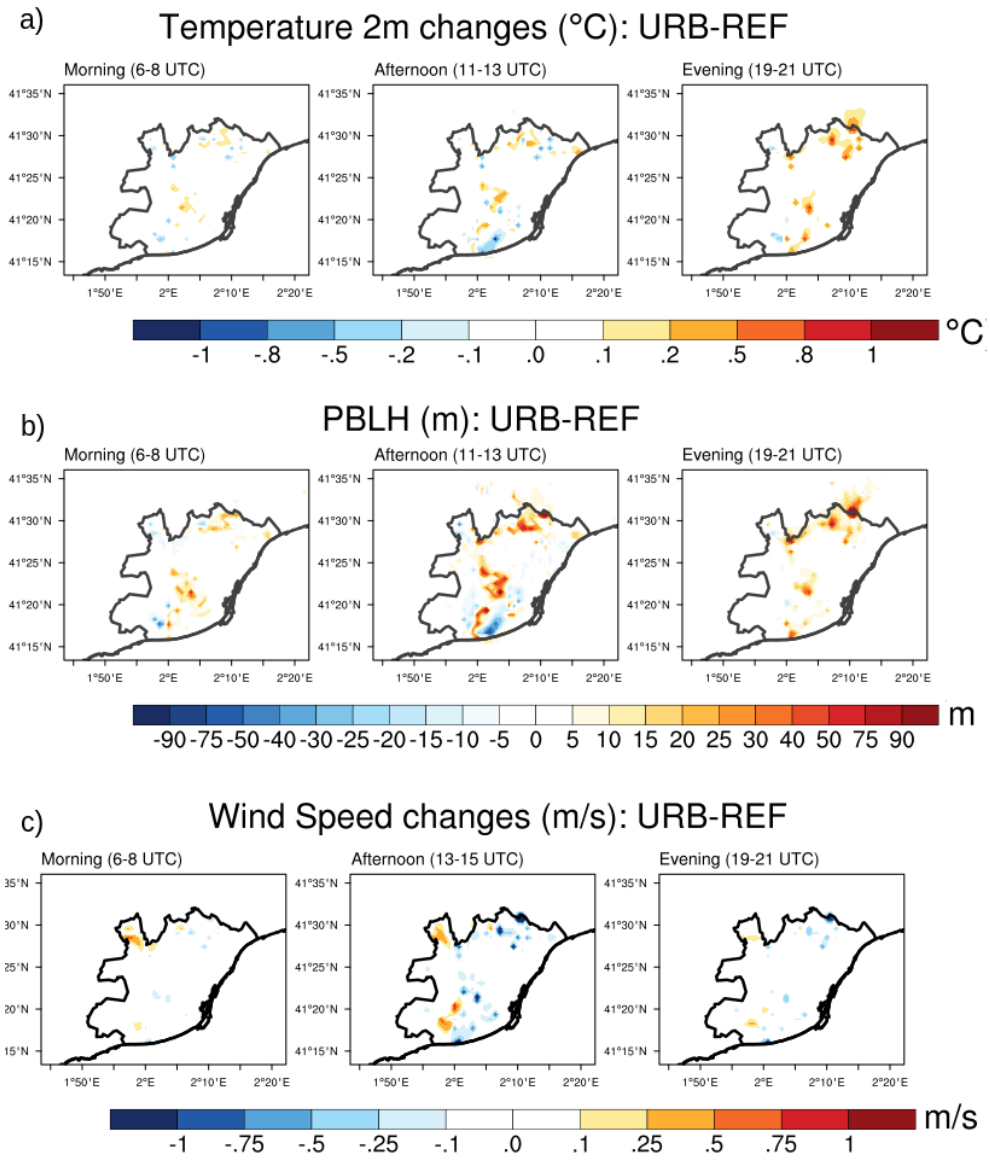

Figure S5: Temperature, PBLH and wind speed changes due to the increase on urbanization (URB-REF).

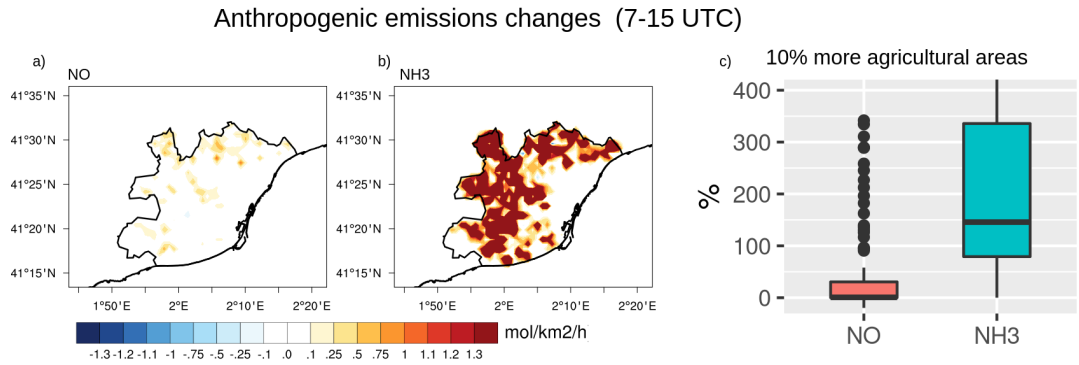

Figure S6: Anthropogenic NO and NH_3 changes due to the increase of agricultural areas (AGR-REF).

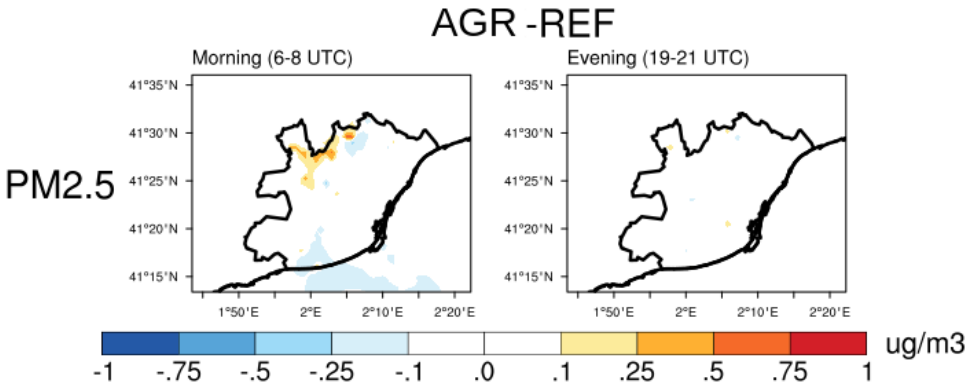

Figure S7: PM2.5 changes es due to the increase of agricultural areas (AGR-REF).

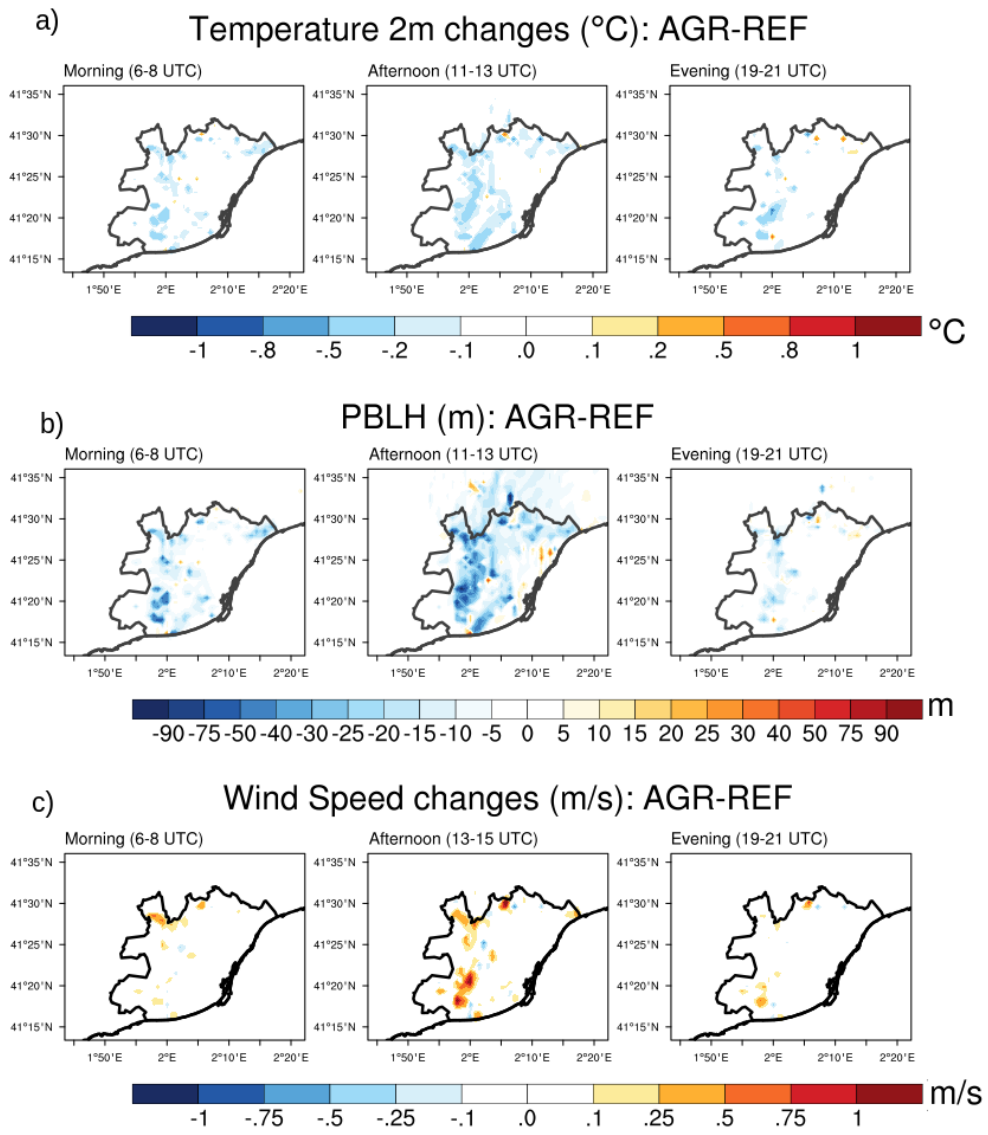

Figure S8: Temperature, PBLH and wind speed changes es due to the increase of agricultural areas (AGR-REF).

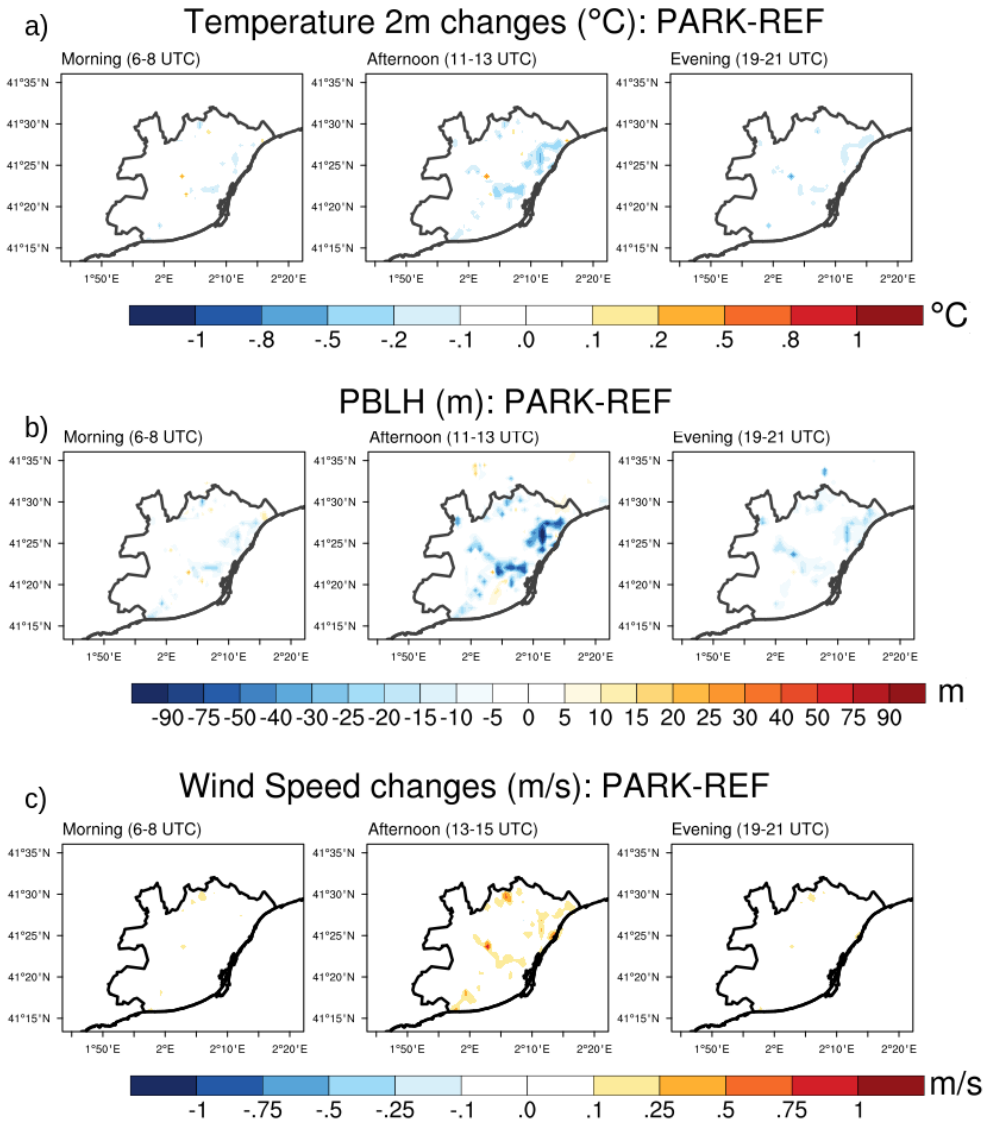

Figure S9: Temperature, PBLH and wind speed changes due to the increase of urban parks (PARK-REF).

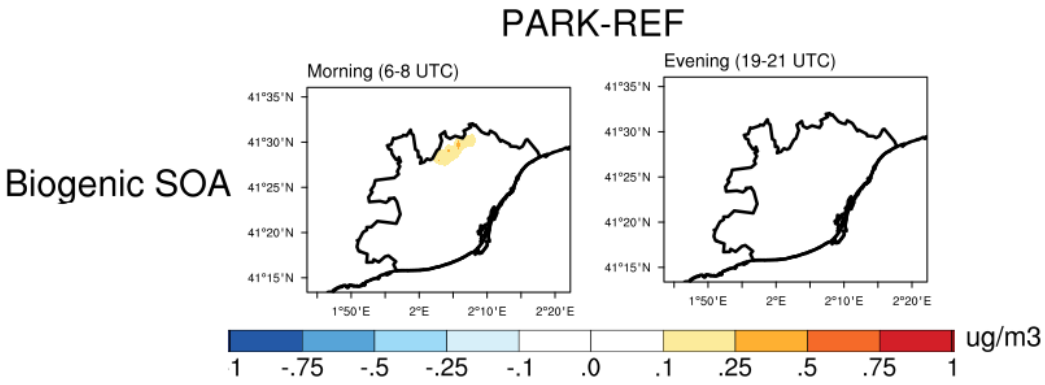

Figure S10: Biogenic SOA changes due to the increase of urban parks (PARK-REF).

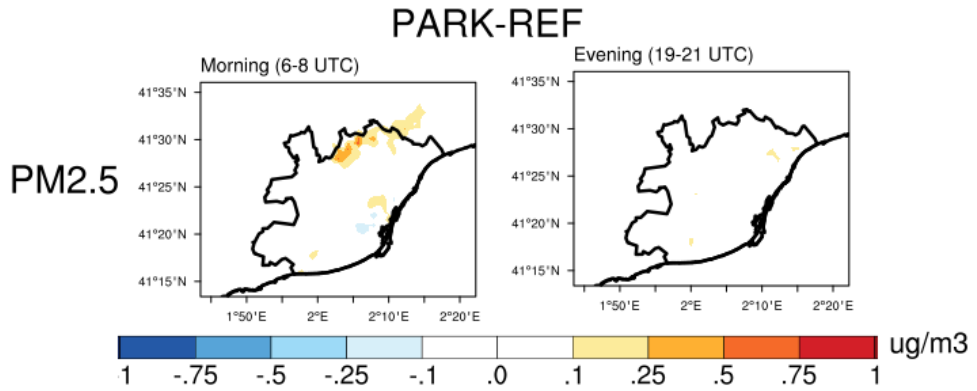

Figure S11: PM2.5 changes due to the increase of urban parks (PARK-REF).

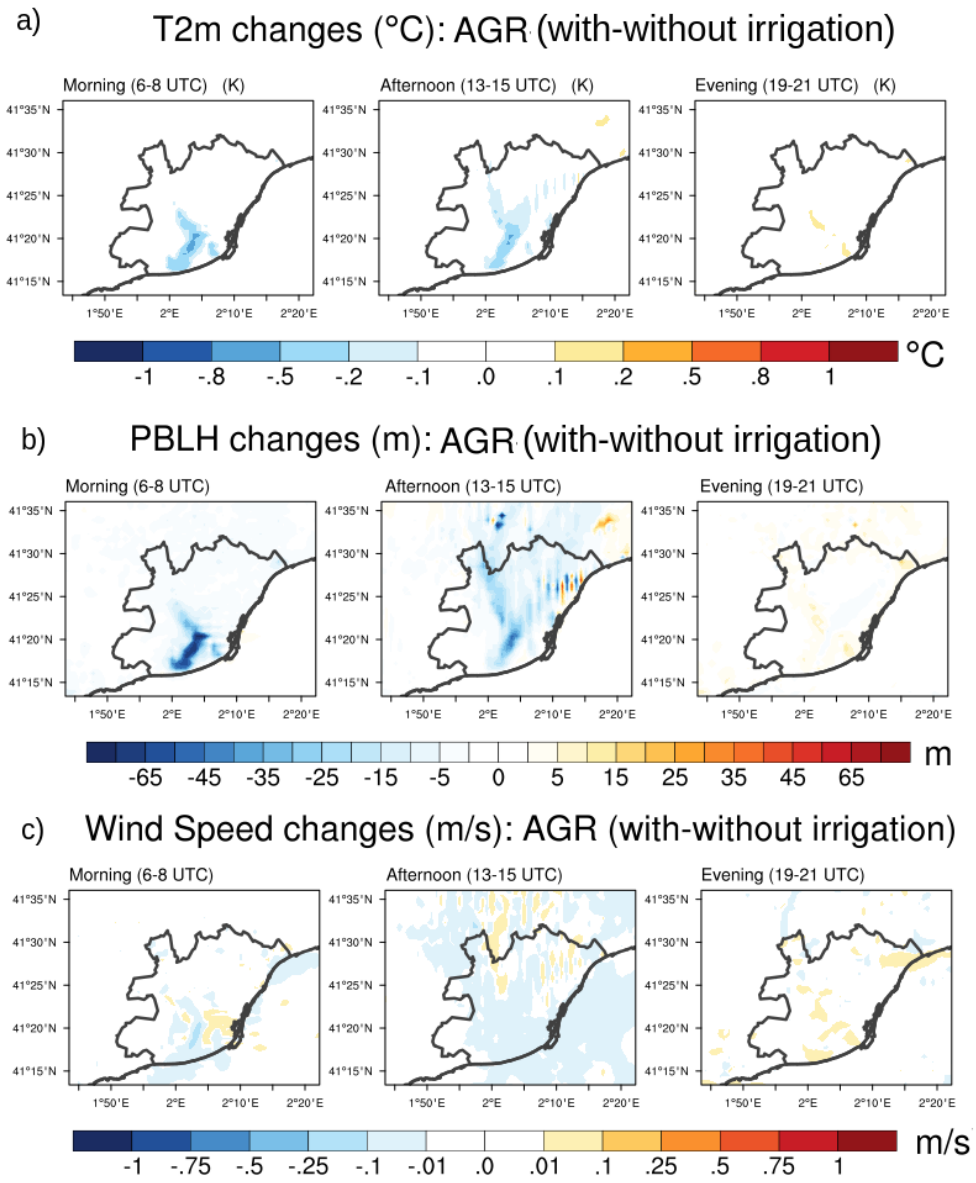

Figure S12: Temperature, PBLH and wind speed changes due to irrigation

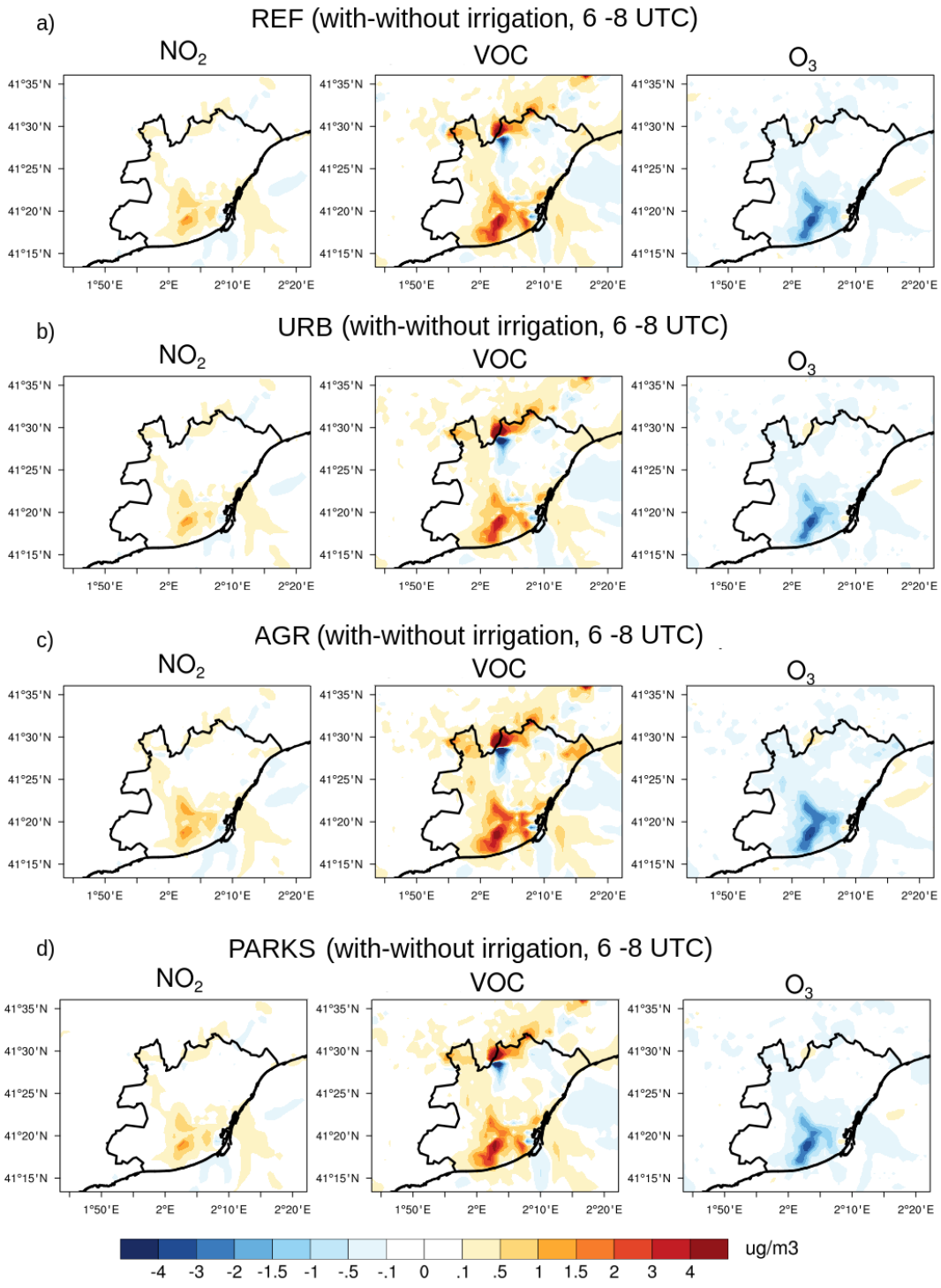

Figure S13: Air quality changes due to irrigation for each scenario.

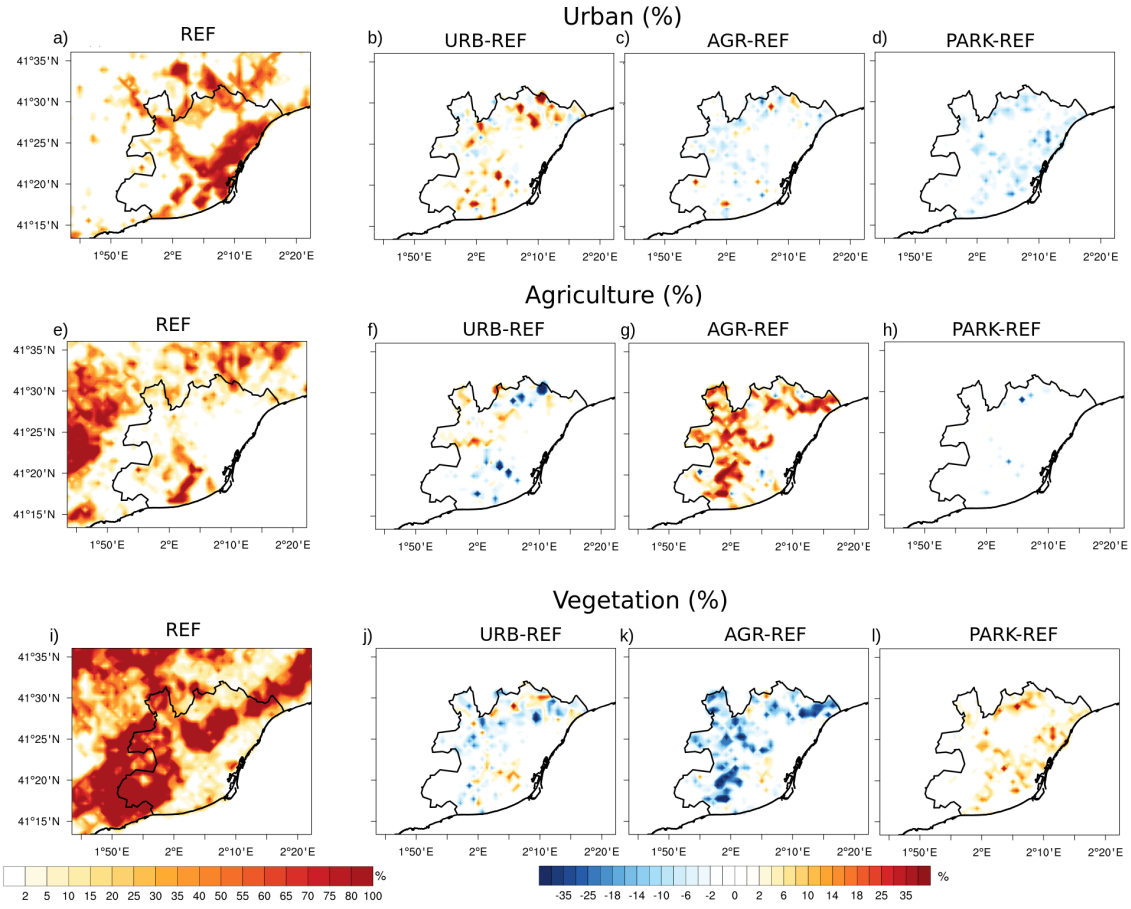

Figure S14: Urban, agriculture, and vegetation fraction for REF, URB-REF and AGR-REF and PARK-REF. Note that urban parks are included in the vegetation percentage.

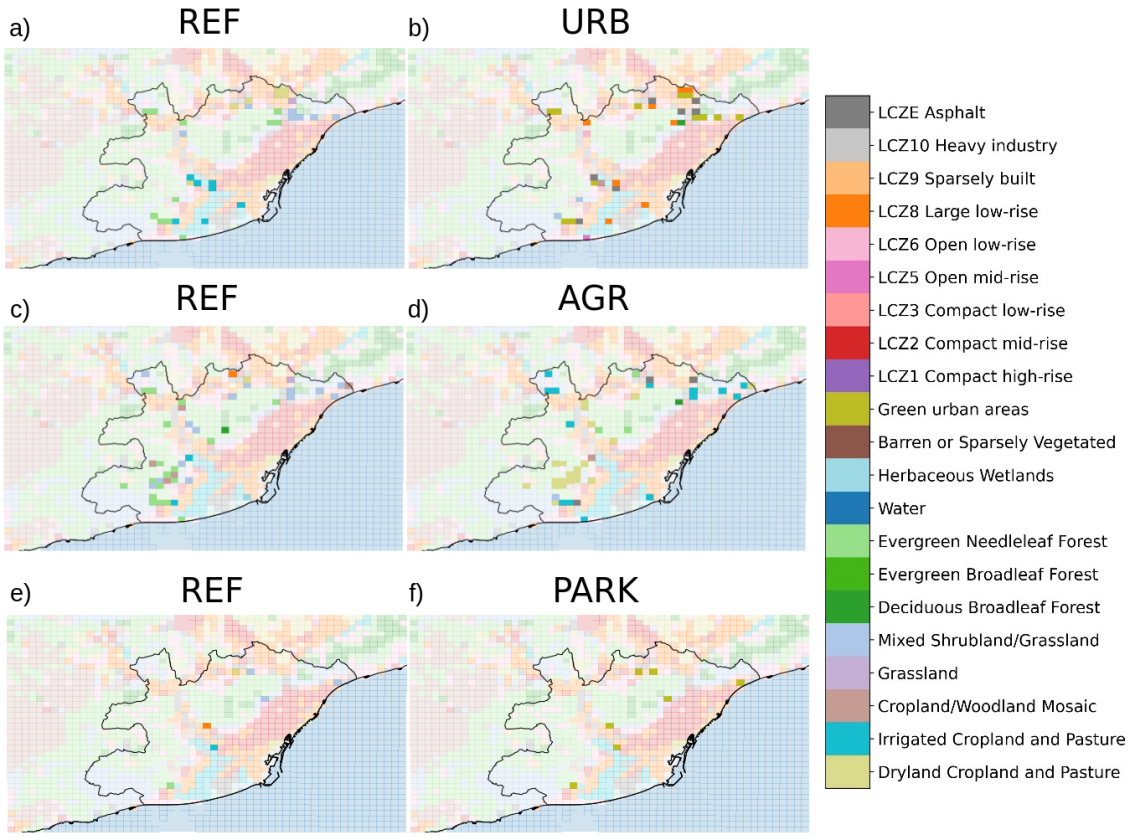

Figure S15: Land-use change between the Urban (URB), agriculture (AGR), and urban parks (PARK) scenarios compared to the reference scenario (REF). Only grids with a change in their land-use are highlighted.

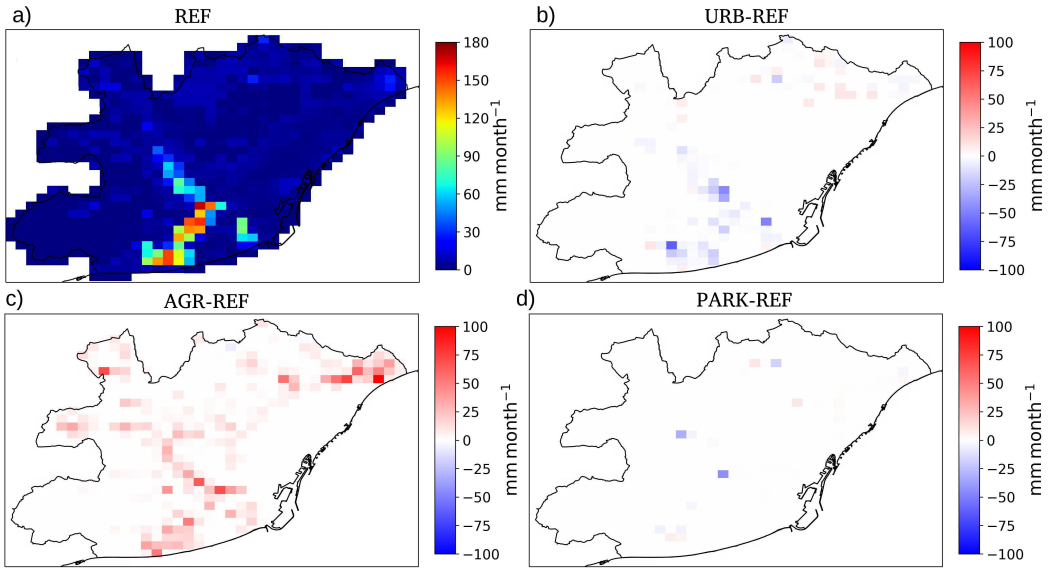

Figure S16: Irrigation for REF and its comparison with the other scenarios: URB, AGR and PARKS scenario for the month of July 2015.

Supplementary Tables

Table S1: Model details and experiment configuration

Chemistry	
Chemical mechanism	RADM2[12]
Aerosol scheme	MADE/SORGAM aerosol scheme[13, 14]
Photolysis scheme	Fast-J[15]
Dry deposition	Wesely scheme[16]
Anthropogenic emissions	HERMES[17]
Biogenic emissions	MEGAN[18]
Physics	
Urban canopy scheme	BEP-BEM [19]
PBL scheme	BouLac [20]
Microphysics	WRF Single-Moment 6-class scheme[21]
Shortwave and longwave radiation	RRTMG scheme[22]
Cumulus (outermost domain)	Kain-Fritsch scheme[23]
Resolution and Initial conditions	
Horizontal resolution	D1: 9 km×9 km, D2: 3km x 3km , D3: 1km x 1km
Vertical layers	45
Top of the atmosphere	100 hPa
Chemical initial condition	WACCM [24]
Meteorological initial condition	ERA5 [25]
Chemistry spin-up	1 month (D1), 10 days (D2, D3)
Time steps	
Physics	18 minutes
Chemistry	18 minutes
Biogenic and Photolysis	30 minutes
Parent ratio	3

Table S2: Statistical evaluation of the modelled meteorology, over the Metropolitan Area of Barcelona (AMB) for July 2015 in hourly basis for the reference scenario (REF). The number of stations are shown in parenthesis on the second column for AMB. The observation mean (OM), model mean (MM), mean bias (MB), normalized mean bias (NMB), root-mean-square error (RMSE) and correlation (R) are calculated between simulated and observed values. Stations are classified into urban and rural. In this evaluation we consider temperature (T), relative humidity (RH), Wind speed (WS) and, Wind direction (WD).

Specie	Type	OM	MM	NMB [0,1]	RMSE	R [0,1]
T (^{o}C)	Urban (10)	27.1	26.9	-0.01	1.4	0.85 – 0.98
	rural (7)	26.2	26.1	-0.01	1.4	0.91 – 0.98
RH (%)	urban (11)	59.5	60.9	0.03	11.7	0.51 – 0.91
	rural (7)	58.8	60.7	0.03	11.5	0.70 – 0.86
WS (m s^{-1})	urban (9)	2.2	1.6	-0.34	1.3	0.66 – 0.91
	rural (7)	2.6	2.9	-0.01	1.3	0.65 – 0.88
WD (^{o})	urban (9)	199.5	191.7	0.00	55.3	0.16 – 0.85
	rural (7)	196.4	201.5	0.01	43.0	0.20 – 0.88

Table S3: Statistical evaluation of the modelled chemistry, over the Metropolitan Area of Barcelona (AMB) for July 2015 in hourly basis for the reference scenario (REF). The number of stations are shown in parenthesis on the second column for AMB. The observation mean (OM), model mean (MM), mean bias (MB), normalised mean bias (NMB), root-mean-square error (RMSE) and correlation (R) are calculated between simulated and observed concentrations. Stations are classified into urban background (urban b.), urban traffic (urban t.), peri-urban background (peri-urban b.), and peri-urban traffic (peri-urban t.).

Specie	Type	OM	MM	NMB [0,1]	RMSE	R [0,1]
NO_2 (µg m^{-3})	urban b. (9)	31.17	30.92	0.001	28.97	0.23 - 0.56
	urban t. (3)	47.36	49.57	0.14	46.43	0.10 - 0.52
	peri-urban. b. (5)	20.17	18.02	-0.11	17.33	0.36 - 0.68
	peri-urban t. (2)	34.30	21.16	-0.37	23.74	0.18 - 0.64
O_3 (µg m^{-3})	urban b. (6)	69.48	72.76	0.06	25.08	0.58-0.77
	urban t. (2)	54.33	61.27	0.13	30.81	0.54-0.62
	peri-urban. b. (4)	74.03	78.18	0.06	25.19	0.58-0.77
	peri-urban t. (1)	71.49	74.06	0.04	25.07	0.70
PM_{10} (µg m^{-3})	urban b. (2)	27.11	7.33	-0.60	21.01	0.01-0.10
	urban t. (2)	36.33	11.89	-0.66	29.30	<0.10
	peri-urban. b. (5)	31.34	9.28	-0.65	26.73	0.2-0.3

References

[1] G. Büttner, B. Kosztra, T. Soukup, A. Sousa, T. Langanke, Clc2018 technical guidelines, 3436, pp. 0–60., Tech. rep. (2017).

[2] J. Gilabert, A. Deluca, D. Lauwaet, J. Ballester, J. Corbera, M. C. Llasat, Assessing heat exposure to extreme temperatures in urban areas using the local climate zone classification, Natural Hazards and Earth System Sciences 21 (1) (2021) 375–391. doi:10.5194/nhess-21-375-2021.
URL https://nhess.copernicus.org/articles/21/375/2021/

[3] J. J. N. Pineda Corresponding author, O. Jorba, J. M. Baldasano, Using noaa avhrr and spot vgt data to estimate surface parameters: application to a mesoscale meteorological model, International Journal of Remote Sensing 25 (1) (2004) 129–143. arXiv:https://doi.org/10.1080/0143116031000115201, doi:10.1080/0143116031000115201.
URL https://doi.org/10.1080/0143116031000115201

[4] R. Segura, A. Badia, S. Ventura, J. Gilabert, A. Martilli, G. Villalba, Sensitivity study of pbl schemes and soil initialization using the wrf-bep-bem model over a mediterranean coastal city, Urban Climate 39 (2021) 100982. doi:https://doi.org/10.1016/j.uclim.2021.100982.
URL https://www.sciencedirect.com/science/article/pii/S2212095521002121

[5] L. S. Pereira, R. G. Allen, M. Smith, D. Raes, Crop evapotranspiration estimation with fao56: Past and future, Agricultural Water Management 147 (2015) 4–20, agricultural Water Management: Priorities and Challenges. doi:https://doi.org/10.1016/j.agwat.2014.07.031.
URL https://www.sciencedirect.com/science/article/pii/S0378377414002315

[6] Agència Catalana de l'aigua (ACA), 2010, Estimació i prognosi de la demanda d'aigua a catalunya. bases tècniques., Tech. rep., Agència de Salut Pública de Barcelona (2010).

[7] Àrea Metropolitana de Barcelona (AMB), 2021, Indicadors socioambientals de la xarxa de parcs metropolitans., Tech. rep., Agència de Salut Pública de Barcelona (2021).

[8] . Ajuntament de Barcelona, Guidelines for irrigation: A practical guide for the irrigation of green areas of barcelona., Tech. rep., Medi Ambient

i Serveis Urbans.
URL https://ajuntament.barcelona.cat/ecologiaurbana

[9] D. Rodriguez-Rey, M. Guevara, M. P. Linares, J. Casanovas, J. Salmerón, A. Soret, O. Jorba, C. Tena, C. Pérez García-Pando, A coupled macroscopic traffic and pollutant emission modelling system for barcelona, Transportation Research Part D: Transport and Environment 92 (2021) 102725. doi:https://doi.org/10.1016/j.trd.2021.102725.
URL https://www.sciencedirect.com/science/article/pii/S1361920921000274

[10] J. Yus-Díez, M. Ealo, M. Pandolfi, N. Perez, G. Titos, G. Močnik, X. Querol, A. Alastuey, Aircraft vertical profiles during summertime regional and saharan dust scenarios over the north-western mediterranean basin: aerosol optical and physical properties, Atmospheric Chemistry and Physics 21 (1) (2021) 431–455. doi:10.5194/acp-21-431-2021.
URL https://acp.copernicus.org/articles/21/431/2021/

[11] C. Reche, N. Pérez, A. Alastuey, N. Cots, E. Pérez, X. Querol, 2011–2020 trends of urban and regional ammonia in and around barcelona, ne spain, Chemosphere 304 (2022) 135347. doi:https://doi.org/10.1016/j.chemosphere.2022.135347.
URL https://www.sciencedirect.com/science/article/pii/S0045653522018409

[12] W. R. Stockwell, P. Middleton, J. S. Chang, X. Tang, The second generation regional acid deposition model chemical mechanism for regional air quality modeling, Journal of Geophysical Research: Atmospheres 95 (D10) (1990) 16343–16367. arXiv:https://agupubs.onlinelibrary.wiley.com/doi/pdf/10.1029/JD095iD10p16343, doi:https://doi.org/10.1029/JD095iD10p16343.
URL https://agupubs.onlinelibrary.wiley.com/doi/abs/10.1029/JD095iD10p16343

[13] I. J. Ackermann, H. Hass, M. Memmesheimer, A. Ebel, F. S. Binkowski, U. Shankar, Modal aerosol dynamics model for europe: development and first applications, Atmospheric Environment 32 (17) (1998) 2981–2999. doi:https://doi.org/10.1016/S1352-2310(98)00006-5.
URL https://www.sciencedirect.com/science/article/pii/S1352231098000065

[14] B. Schell, I. J. Ackermann, H. Hass, F. S. Binkowski, A. Ebel, Modeling the formation of secondary organic aerosol within a

comprehensive air quality model system, Journal of Geophysical Research: Atmospheres 106 (D22) (2001) 28275–28293. doi:https://doi.org/10.1029/2001JD000384.
URL https://agupubs.onlinelibrary.wiley.com/doi/abs/10.1029/2001JD000384

[15] O. Wild, X. Zhu, M. J. Prather, Journal of Atmospheric Chemistry 37 (3) (2000) 245–282. doi:10.1023/a:1006415919030, [link].
URL https://doi.org/10.1023/a:1006415919030

[16] M. Wesely, Parameterization of surface resistances to gaseous dry deposition in regional-scale numerical models, Atmospheric Environment 41 (2007) 52–63. doi:https://doi.org/10.1016/j.atmosenv.2007.10.058.
URL https://www.sciencedirect.com/science/article/pii/S1352231007009740

[17] M. Guevara, C. Tena, M. Porquet, O. Jorba, C. Pérez García-Pando, Hermesv3, a stand-alone multi-scale atmospheric emission modelling framework – part 2: The bottom–up module, Geoscientific Model Development 13 (3) (2020) 873–903. doi:10.5194/gmd-13-873-2020.
URL https://gmd.copernicus.org/articles/13/873/2020/

[18] A. B. Guenther, X. Jiang, C. L. Heald, T. Sakulyanontvittaya, T. Duhl, L. K. Emmons, X. Wang, The model of emissions of gases and aerosols from nature version 2.1 (megan2.1): an extended and updated framework for modeling biogenic emissions, Geoscientific Model Development 5 (6) (2012) 1471–1492. doi:10.5194/gmd-5-1471-2012.
URL https://gmd.copernicus.org/articles/5/1471/2012/

[19] F. Salamanca, A. Martilli, M. Tewari, F. Chen, A study of the urban boundary layer using different urban parameterizations and high-resolution urban canopy parameters with WRF, Journal of Applied Meteorology and Climatology 50 (5) (2011) 1107–1128. doi:10.1175/2010jamc2538.1.
URL https://doi.org/10.1175/2010jamc2538.1

[20] P. Bougeault, P. Lacarrere, Parameterization of orography-induced turbulence in a mesobeta–scale model, Monthly Weather Review 117 (8) (1989) 1872 – 1890. doi:10.1175/1520-0493(1989)117¡1872:POOITI¿2.0.CO;2.

[21] S.-Y. Hong, J.-h. Kim, J.-o. Lim, J. Dudhia, The wrf single moment microphysics scheme (wsm), Journal of the Korean Meteorological Society 42 (2006) 129–151.

[22] M. J. Iacono, J. S. Delamere, E. J. Mlawer, M. W. Shephard, S. A. Clough, W. D. Collins, Radiative forcing by long-lived greenhouse gases: Calculations with the aer radiative transfer models, Journal of Geophysical Research: Atmospheres 113 (D13) (2008). doi:https://doi.org/10.1029/2008JD009944.
URL https://agupubs.onlinelibrary.wiley.com/doi/abs/10.1029/2008JD009944

[23] J. S. Kain, The kain–fritsch convective parameterization: An update, Journal of Applied Meteorology 43 (1) (2004) 170–181. doi:10.1175/1520-0450(2004)043¡0170:tkcpau¿2.0.co;2.
URL http://dx.doi.org/10.1175/1520-0450(2004)043<0170:TKCPAU>2.0.CO;2

[24] A. Gettelman, M. J. Mills, D. E. Kinnison, R. R. Garcia, A. K. Smith, D. R. Marsh, S. Tilmes, F. Vitt, C. G. Bardeen, J. McInerny, H.-L. Liu, S. C. Solomon, L. M. Polvani, L. K. Emmons, J.-F. Lamarque, J. H. Richter, A. S. Glanville, J. T. Bacmeister, A. S. Phillips, R. B. Neale, I. R. Simpson, A. K. DuVivier, A. Hodzic, W. J. Randel, The whole atmosphere community climate model version 6 (waccm6), Journal of Geophysical Research: Atmospheres 124 (23) (2019) 12380–12403. doi:https://doi.org/10.1029/2019JD030943.
URL https://agupubs.onlinelibrary.wiley.com/doi/abs/10.1029/2019JD030943

[25] H. Hersbach, B. Bell, P. Berrisford, S. Hirahara, A. Horányi, J. Muñoz-Sabater, J. Nicolas, C. Peubey, R. Radu, D. Schepers, A. Simmons, C. Soci, S. Abdalla, X. Abellan, G. Balsamo, P. Bechtold, G. Biavati, J. Bidlot, M. Bonavita, G. De Chiara, P. Dahlgren, D. Dee, M. Diamantakis, R. Dragani, J. Flemming, R. Forbes, M. Fuentes, A. Geer, L. Haimberger, S. Healy, R. J. Hogan, E. Hólm, M. Janisková, S. Keeley, P. Laloyaux, P. Lopez, C. Lupu, G. Radnoti, P. de Rosnay, I. Rozum, F. Vamborg, S. Villaume, J.-N. Thépaut, The era5 global reanalysis, Quarterly Journal of the Royal Meteorological Society 146 (730) (2020) 1999–2049. doi:https://doi.org/10.1002/qj.3803.
URL https://rmets.onlinelibrary.wiley.com/doi/abs/10.1002/qj.3803